

communication) that the equations-of-motion method [D. J. Rowe, *Rev. Mod. Phys.* **40**, 153 (1968)] gives rise to relations of the form (III. 7b) and (III. 10) but having greater general validity than the usual RPA.

⁶F. Villars, in *Nuclear Physics, Proceedings of the International School of Physics "Enrico Fermi," Course XXIII*, edited by V. F. Weisskopf (Academic, New York, 1963).

⁷E. R. Marshalek and J. Weneser, *Ann. Phys. (N.Y.)* **53**, 569 (1969).

⁸E. R. Marshalek and J. Weneser, *Phys. Rev. C* **2**, 1682 (1970).

⁹E. R. Marshalek and G. Holzwarth, *Nucl. Phys.* **A191**, 438 (1972).

¹⁰A. Mann and I. Unna, *Phys. Lett.* **27B**, 72 (1968).

¹¹Only the Y_{20} components of the residual interaction enter into the calculation.

¹²I. Hamamoto, *Nucl. Phys.* **A177**, 484 (1971).

¹³Divergences on both sides of the sum cancel to give a finite result.

¹⁴B. L. Birbrair and K. N. Nikolaev, *Yad. Fiz.* **14**, 705

(1971) [*Sov. J. Nucl. Phys.* **14**, 397 (1972)].

¹⁵N. I. Pyatov and M. I. Chernei, Joint Institute for Nuclear Research Report No. P4-6367, 1972 (to be published).

¹⁶E. R. Marshalek, *Phys. Rev. C* **3**, 1710 (1971).

¹⁷E. R. Marshalek and M. Sabato, *Phys. Rev. C* **5**, 1130 (1972).

¹⁸R. A. Broglia, R. Liotta, and V. Paar, *Phys. Lett.* **38B**, 480 (1972).

¹⁹E. R. Marshalek, *Nuovo Cimento Lett.* **4**, 631 (1972).

²⁰D. R. Bes and R. A. Sorensen, *Advances in Nuclear Physics*, (Plenum, New York, 1968), Vol. 2, p. 129.

²¹E. R. Marshalek, *Phys. Rev.* **139**, B770 (1965).

²²E. R. Marshalek, *Phys. Rev.* **158**, 993 (1967).

²³I. M. Pavlichenkov, *Nucl. Phys.* **55**, 225 (1964).

²⁴O. Mikoshiba, R. K. Sheline, T. Udagawa, and S. Yoshida *Nucl. Phys.* **A101**, 202 (1967).

²⁵Ironically, the underestimate appears to improve agreement with experiment, at least when the pairing and quadrupole-quadrupole force is used.

Errors on Charge Densities Determined from Electron Scattering*

J. Borysowicz and J. H. Hetherington

Physics Department and Cyclotron Laboratory, Michigan State University, East Lansing, Michigan 48823

(Received 19 March 1973)

Errors on the charge distribution as derived from electron scattering are determined and they depend largely on assumptions about the possible large- q behavior of the form factor (i.e., at larger- q values than have been measured). We use rather general expansions for $\rho(r)$, for example the cosine series or a set of spline functions. We find the charge distribution and its error to be not very dependent on the set of functions used for expansion but dependent instead on assumptions about and knowledge of the errors in $f(q)$. Charge densities and their errors for ${}^3\text{He}$ and ${}^4\text{He}$ based on electron scattering are shown.

1. INTRODUCTION

The charge density is assumed to be a linear series using quite general sets of functions. This allows study of the errors in the determination of $\rho(r)$. The functions used are, for example, the cosine series or sets of spline functions. We have investigated a large number of other sets but find that the results are rather independent of the set used provided it meets rather general criteria. Our error analysis makes use of the error matrix of the coefficients of the series. The error matrix can be diagonalized by transforming to a new set of basis functions for expansion. In this form the errors on the coefficients of the series are uncorrelated. This formulation leads to considerable conceptual simplification of the error statement.

We find that in electron scattering experiments, where $f(q)$ is only measured out to some q_{max} , that

the error in $\rho(r)$ is not well defined unless we use a rather restricted set of functions. However, it becomes well defined and of reasonable magnitude for a less restricted set of functions when some weak limits are assumed on the form factor in the high- q region where there are no measurements. In this paper application of the method has been made only to systems which can be treated in Born approximation. Therefore, we have studied only ${}^3\text{He}$ and ${}^4\text{He}$ elastic electron scattering as examples of the techniques described. The methods, as we show, can easily be applied to any (higher- Z) nucleus by straightforward application of any scattering code suitable for calculation of the cross section from the charge distributions.

Sections 2-5 give a derivation of the method. There is little or none here that is new from a mathematical standpoint, but it is included in order to clarify exactly what we do and to clearly define and distinguish between the ideas of the

measured quantities (experiment space) and the class of functions (model space) which must be used for the expansion of $\rho(r)$. Section 6 applies the theory of the preceding sections to the analysis of the charge distribution of ^3He and ^4He and a determination of the errors in those charge distributions.

2. EXPERIMENT SPACE

The measurements f_i which are made are assumed to be related to the true charge distribution by the form

$$f_i^0 = \int_0^\infty \mathcal{E}_i(r) \rho(r) dr, \quad (2.1)$$

where $\rho(r)$ is the charge distribution and where the $\mathcal{E}_i(r)$ are a set of functions which characterize the measurements. The measured quantities f_i will differ from f_i^0 because of measurement errors. In electron scattering in Born approximation we have

$$\mathcal{E}_i(r) = 4\pi r^2 j_0(q_i r), \quad (2.2)$$

where j_0 is the spherical Bessel function and where the factor $4\pi r^2$ comes from the weight function of the three-dimensional integration. With this choice of \mathcal{E}_i the f_i is the form factor at the momentum transfer q_i . Functions \mathcal{E}_i can also be introduced to specify the mean squared radius and/or other measured quantities which one wishes to introduce into the fitting process. The \mathcal{E}_i can be modified to incorporate finite experimental angular resolution if one desires.

The set of N measured quantities therefore leads us to a set of N functions $\mathcal{E}_i(r)$, $1 \leq i \leq N$. This set of functions will be referred to as the *experiment space*.

In case Born approximation is not valid so that the measured quantities are not linear functions of the charge distribution,¹ we may linearize the problem by considering deviations from a charge distribution which almost fits the data. Any of the many functional forms already being used to fit charge distributions can be used as a sort of base charge which we will call $\rho_0(r)$. Then if there are measurements of cross section related to the charge distribution by some nonlinear functional $\sigma_i = F\{\rho(r)\}$ we can assume that if we take as measurements

$$\Delta\sigma_i = \sigma_i(\text{measured}) - \sigma_i(\text{base}),$$

we can linearize the functional F and we obtain

$$\begin{aligned} \Delta\sigma_i &= F_i\{\rho(r)\} - F_i\{\rho_0(r)\} \\ &= \int_0^\infty \left. \frac{\delta F_i\{\rho(r)\}}{\delta\rho(r)} \right|_{\rho_0(r)} D\rho(r) dr, \end{aligned}$$

where

$$D(r) = \rho(r) - \rho_0(r).$$

Therefore, in all we say below the functions

$$\left. \frac{\delta F_i}{\delta\rho} \right|_{\rho_0}$$

are to be used instead of $\mathcal{E}_i(r)$ and the function $D(r)$ instead of $\rho(r)$ and $\Delta\sigma_i$ instead of f_i if we are to apply the derivation to situations where Born approximation is not valid.

3. MODEL SPACE

If there would be no practical limitations on the design of the experiment, one would select an experiment with such $\mathcal{E}_i(r)$ and N that

$$\rho(r) = \sum_{i=1}^N e_i \mathcal{E}_i(r) \quad (3.1)$$

would hold and coefficients e_i would be easily determined by the least-squares fit. Usually the experiment itself is not sufficient to determine the density and consequently (3.1) is *not true*.

Some information additional to that obtained from the experiment is required to make the determination of the density possible.

An example of such information is our belief that density is a reasonably "smooth" function and has a certain, let us say "exponential," behavior in the tail region. This has led to assumptions of specific functional shapes for the density. There are many such shapes in the literature,² an example being the celebrated Fermi distribution and its variations. In general, by a judicious choice of the shape a good fit is obtained. The procedure is open to the charge of arbitrariness,³ especially when one is looking for fine structure ("wiggles") in the density.

We shall show how to determine $\rho(r)$ under very weak assumptions about (a) the functional form of $\rho(r)$ and (b) behavior of the form factor at large q 's. We shall consider M states (functions) $\mathfrak{M}_m(r)$ which define a M -dimensional model space. They are used to expand $\rho(r)$:

$$\rho(r) = \sum_{m=1}^M a_m \mathfrak{M}_m(r). \quad (3.2)$$

The model space can be used now to incorporate information about the charge density that is not determinable from the measurements taken.

There are two obvious properties of this kind: (a) The density has no cusp at origin; and (b) the density goes to zero outside some radius r_0 large compared with the nuclear radius. A stronger version of the condition (a) states: The density has all odd derivatives zero at the origin. This strong-

er version is fulfilled in the case of the cosine-model space [see Eq. (6.1)]. For other model spaces we did not use property (a) at all. Property (b) has been incorporated into all model spaces we used by assuming for each model state:

$$\mathfrak{N}_m(r) = 0 \quad \text{for } r > r_0. \quad (3.3)$$

In the cases we considered r_0 is smaller than the maximum distance probed by the experiment:

$$r_{\max} = \pi/\Delta q, \quad (3.4)$$

where Δq is the experimental increment in momentum transfer. Therefore, (3.3) is equivalent to asking for a smooth interpolation for the form factor between its measured values f_i .

In the following part of this section we present further less rigorous guidelines for the selection of model states.

The property of "smoothness" of the density is difficult to deal with. We do not know well how many derivatives of the density should exist and what their bounds are. However the experimental resolution in radius is given by⁴

$$\Delta r = \pi/q_{\max}, \quad (3.5)$$

where q_{\max} is the maximum measured momentum transfer. On a length scale shorter than this the experiment gives no information about the smoothness. A natural and convenient way to introduce additional assumptions about the smoothness of $\rho(r)$ is to assume upper bounds on the form factor outside of the measured region (i.e., for $q > q_{\max}$). This will be discussed in detail in Sec. 6.

Besides this assumption about f_i , implicit assumptions about smoothness are made depending on the smoothness of the model states $\mathfrak{N}_m(r)$ used. In Sec. 6 we consider a variety of model spaces from the very smooth cosine space through splines to very unsmooth unspline spaces. It is encouraging that results do not depend crucially on the choice of the model space.

An important characteristic of the model space is its dimension M . By combining (3.4) and (3.5) we obtain for the number of experimentally resolved regions:

$$M \approx q_{\max} r_0 / \pi. \quad (3.6)$$

This equation gives a practical estimate of the maximum number of independent functions which contribute to $f(q)$ mainly in the region $q < q_{\max}$ and are zero outside of r_0 . We shall see in Sec. 6 that the maximum number of states that is determinable from experiment agrees well with (3.6).

Because model spaces are finite the expansion (3.2) is not always true. We therefore distinguish between a *good* model space and one that is *not good*. A *good* model space is one for which the

expansion (3.2) holds while for a *not-good* model space (3.2) is not exact. In other words, a *good model space contains the charge density*.

Consider a model space M . After an experiment is performed we may find out that M is not good (because χ^2 is not low enough, see Sec. 6). If this is not the case it is not proved, however, that the model space is good; another experiment (with greater precision or greater range of q values) could show M to be not good. We summarize: It is possible to show experimentally (on the basis of χ^2) that a model space is not good. It is not possible using a finite experiment to verify that a model space is good. This is equivalent to saying that an infinite chain of measurements is necessary to find the density exactly.

4. MEASUREMENT ERRORS AND DENSITY

In this and in the next section we shall derive errors in the determination of the density assuming that the model space we use is good. The errors determined will depend not only on the measurement errors but also on the model space used. They will increase with the dimension M of the model space. We must keep, however, the dimension M sufficiently large to be sure that the model space is good.

The measurements f_i are not exact but are known to some accuracy σ_i (not to be confused with the cross section σ used in Sec. 2). That is, there is assumed to be a normal distribution of possible values f_i given by

$$P(f_i) = \exp[-(f_i - f_i^0)^2 / 2\sigma_i^2]. \quad (4.1)$$

Furthermore, the joint probability of all measurements having a given set of values $\{f_i\}$ is given by:

$$P(\{f_i\}) = e^{-\chi^2/2}, \quad (4.2)$$

where

$$\chi^2 = \sum_{i=1}^N (f_i - f_i^0)^2 / \sigma_i^2. \quad (4.3)$$

Since we assume that the model space is good we may write, using Eq. (3.2):

$$f_i^0 = \sum_m \int_0^\infty \mathcal{E}_i(r) \mathfrak{N}_m(r) dr a_m. \quad (4.4)$$

We may then minimize χ^2 by varying the a_m . This is a simple least-squares minimization.

Introducing the definition⁵

$$P_{i_m} \equiv \int_0^\infty \mathcal{E}_i(r) \mathfrak{N}_m(r) dr \quad (4.5)$$

we obtain, from the conditions $\partial\chi^2/\partial a_m = 0$ that the

a_m which minimize χ^2 are solutions of the equation

$$\sum_{m=1}^M M_{nm} a_m^e = G_n, \quad (4.6)$$

where the error matrix is defined by

$$M_{nm} \equiv \sum_{i=1}^N \frac{P_{in} P_{im}}{\sigma_i^2} \quad (4.7)$$

and where,

$$G_n = \sum_{i=1}^N \frac{f_i P_{in}}{\sigma_i^2}. \quad (4.8)$$

In Eq. (4.6) the superscript e on the a^e indicates that it is derived from experiment. The most probable charge distribution corresponding to experiment, $\rho^e(r)$, is given by

$$\rho^e(r) = \sum_{m=1}^M \mathfrak{N}_m(r) a_m^e. \quad (4.9)$$

The distribution of coefficients $a_m = a_m^e + \Delta a_m$ is given by

$$P\{\Delta a_m\} = C e^{-\chi^2 \Delta^2 / 2}, \quad (4.10)$$

where C is a normalization and where

$$\chi^2 \Delta^2 = \chi^2_0 + \sum_{m,n=1}^M \Delta a_n \Delta a_m M_{nm}. \quad (4.11)$$

Here χ^2_0 is the minimum value of χ^2 , i.e., corresponding to $a_m = a_m^e$. Since these errors are coupled it is useful to obtain new functions $\mathfrak{W}_m(r)$ which are linear combinations of the $\mathfrak{N}_m(r)$ and which correspond to a diagonal error matrix. To do this we may use the orthogonal transformation which diagonalizes M_{nm}

$$\sum_{n,m} U_{nk} M_{nm} U_{ml} = \delta_{kl} D_k. \quad (4.12)$$

Then defining

$$b_k \equiv \sum_n U_{nk} a_n^e, \quad (4.13)$$

$$\Delta b_k \equiv \sum_n U_{nk} \Delta a_n,$$

we have

$$\chi^2 = \chi^2_0 + \sum_k D_k (\Delta b_k)^2. \quad (4.14)$$

Transforming the basis of the model space we obtain the functions

$$\mathfrak{W}_i(r) = \sum_m \mathfrak{N}_m(r) U_{mi}. \quad (4.15)$$

The charge distribution which corresponds to the values Δb_m is

$$\rho(r) = \rho^e(r) + \sum_k \mathfrak{W}_k(r) \Delta b_k, \quad (4.16)$$

while its probability is given by

$$P\{\Delta b_k\} = \exp\left[-\sum_k \frac{1}{2} D_k (\Delta b_k)^2\right]. \quad (4.17)$$

Therefore one standard deviation in b_k is given by

$$D_k^{-1/2}. \quad (4.18)$$

Therefore adding any one of the functions

$$\mathfrak{W}_k(r) D_k^{-1/2} \quad (4.19)$$

to the experimental distribution $\rho^e(r)$ changes χ^2 by 1 standard deviation. This gives a convenient way of exploring the charge densities permitted by experiment.

Because the errors on the coefficients b are uncorrelated we may compute the error at any one point on $\rho(r)$ as the square root of the sum of the squares of the individual error contributions (4.19). Therefore

$$\Delta\rho(r) = \left[\sum_k \mathfrak{W}_k^2(r) D_k^{-1} \right]^{1/2}, \quad (4.20)$$

where $\Delta\rho(r)$ is the error in the estimation (4.9) of $\rho(r)$. This error $\Delta\rho(r)$ is of course not uncorrelated to errors in ρ at other values of r . It is, however, extremely useful to have this error quantity. It answers the question: What is the uncertainty in our knowledge of $\rho(r_0)$ at a single given r_0 on the basis of a given experiment and with certain model assumptions? The error correlations are, of course, also quite important and instructive. They are treated in the next section.

We summarize: *If the model space is good then the experiment determines the charge density $\rho^e(r) \pm \Delta\rho(r)$.*⁶

5. CORRELATED ERRORS IN THE CHARGE DENSITY

For convenience in what follows it is useful to change the normalization of the functions $\mathfrak{W}_m(r)$ so that the diagonal error matrix becomes the Kronecker δ . This is accomplished by defining:

$$C_m(r) = D_m^{-1/2} \mathfrak{W}_m(r).$$

There is only one requirement on the functions C_m , that they are orthonormal with respect to the error matrix. Therefore any orthogonal transformation on C_m 's will provide another equivalent set of functions.

We introduce coefficients:

$$d_m = D_m^{1/2} b_m \quad (5.1)$$

so that:

$$\rho^e(r) = \sum_m d_m C_m(r). \quad (5.2)$$

The normalization is such that the standard errors on the coefficient d_m are unity, as is evident

from Eqs. (5.1) and (4.19), and $\Delta\rho(r)$ takes the form

$$\Delta\rho(r) = \left[\sum_n C_n^2(r) \right]^{1/2}. \quad (5.3)$$

We shall determine now a change $\delta\rho(r_2)$ from the most probable value $\rho^e(r_2)$ when $\rho(r_1)$ is changed from its most probable value $\rho^e(r_1)$ by $\delta\rho(r_1)$. To do that we shall seek an orthogonal transformation U_{mn} such that the new basis functions C'_m have the property

$$C'_m(r_1) = \sum_n U_{mn} C_n(r_1) = \delta_{1m} C'_1(r_1) \quad (5.4)$$

and therefore:

$$\rho^e(r_1) = d'_1 C'_1(r_1)$$

and

$$\rho^e(r_2) = d'_1 C'_1(r_2) + \sum_{m=2} d'_m C'_m(r_2).$$

Because errors on d'_m are uncorrelated:

$$\delta\rho(r_2) = \frac{C'_1(r_2)}{C'_1(r_1)} \delta\rho(r_1).$$

U_{1n} is found from (5.4)

$$U_{1n} = C_n(r_1) / \left[\sum C_n^2(r_1) \right]^{1/2} = C_n(r_1) / \Delta\rho(r_1) \quad (5.5)$$

and therefore

$$C'_1 = \Delta\rho(r_1).$$

Finally,

$$\delta\rho(r_2) = \frac{C'_1(r_2)}{\Delta\rho(r_1)} \delta\rho(r_1).$$

The error in $\rho(r_2)$ will also be changed because we have effectively added a constraint by specifying $\rho(r_1)$. Now because the uncorrelated error $\Delta\rho(r_2)$ is given by

$$\Delta\rho(r_2) = \left[\sum_m C_m^2(r_2) \right]^{1/2} = \left[\sum_m C_m'^2(r_2) \right]^{1/2} \quad (5.6)$$

and because the constraint merely eliminates the contribution of the function $C'_1(r)$ from the error in $\rho(r)$ we may write

$$\Delta\rho(r_2) = \left\{ [\Delta\rho(r_2)]^2 - [C'_1(r_2)]^2 \right\}^{1/2}.$$

The results obtained above can be written in a more symmetric way if we write the variations as fractions of uncorrelated errors $\Delta\rho(r_1)$ and $\Delta\rho(r_2)$. We obtain

$$\frac{\delta\rho(r_2)}{\Delta\rho(r_2)} = g(r_2, r_1) \times \frac{\delta\rho(r_1)}{\Delta\rho(r_1)} \pm [1 - g^2(r_2, r_1)]^{1/2}, \quad (5.7)$$

where

$$g(r_2, r_1) = \frac{C'_1(r_2)}{\Delta\rho(r_2)} = \frac{\sum_m C_m(r_1) C_m(r_2)}{\Delta\rho(r_1) \Delta\rho(r_2)}, \quad (5.8)$$

where Eqs. (5.4) and (5.5) have been used for the very last step. We will call the quantity $g(r_2, r_1)$ the correlation function.

In words we can say: *The deviation of $\rho(r_2)$ from $\rho^e(r_2)$ as a fraction of the error $\Delta\rho(r_2)$ due to a constraint of $\rho(r_1)$ to a deviation $\delta\rho(r_1)$ expressed as a fraction of $\Delta\rho(r_1)$ is simply the correlation function g times the fractional deviation of $\rho(r_1)$. The error $\Delta\rho(r_2)$ is reduced by the factor $(1 - g^2)^{1/2}$ as a result of the constraint.*

It is easily seen from Eqs. (5.8) and (5.6) that $g(r_2, r_1)$ cannot be greater than 1. When g is very close to 1 or -1 then strong correlations in the errors are implied.

6. CHARGE DISTRIBUTION OF ${}^3\text{He}$ AND ${}^4\text{He}$

To illustrate these considerations we have studied the ${}^3\text{He}$ electron scattering data of Sick and McCarthy.⁷ We include as data the value $f(0) = 1 \pm 0.0001$. The effects of experimental resolution have not been included. We first use the M -dimensional cosine model spaces

$$\mathfrak{H}_m(r) = \begin{cases} \cos[(m - \frac{1}{2})(\pi/r_0)r] & \text{if } r < r_0 \\ 0 & \text{if } r \geq r_0 \end{cases} \quad (6.1)$$

for $1 \leq m \leq M$ and we try several values of M . r_0 is chosen reasonably large, i.e., $r_0 = 5$ fm. Figure 1 shows χ^2 and the error $\Delta\rho(0)$ in the value of $\rho(0)$ as a function of M for the ${}^3\text{He}$ data.

We find that for $M < 7$ the value of χ^2 is outside and above its normal region

$$\chi_{\text{normal}}^2 = N - 1 \pm [2(N - 1)]^{1/2}, \quad (6.2)$$

where N is the number of degrees of freedom. Therefore, expansion (3.2) is not true and the cosine spaces (6.1) with $M < 7$ are not good. For $M = 7$ or 8 , χ^2 reaches the normal region (6.2) and we have a model space which cannot be shown to be not good. At the same time $\Delta\rho(0)$ is finite which shows that all coefficients a_m in (3.2) are determined. The charge distribution corresponding to this situation is so similar to Fig. 4 that we have not shown it separately. For $M > 8$ we find that $\Delta\rho(0)$ suddenly becomes very large [compared to $\rho(0)$], while χ^2 drops somewhat lower than might be required by statistical considerations. The value of M for which $\Delta\rho$ diverges agrees well with the value obtained from Eq. (3.6): $M = 5 \times 4.5/\pi = 7.2$. The transforms of the first seven or eight cosines overlap the region $0 - q_{\text{max}}$ enough so that their coefficients can be deter-

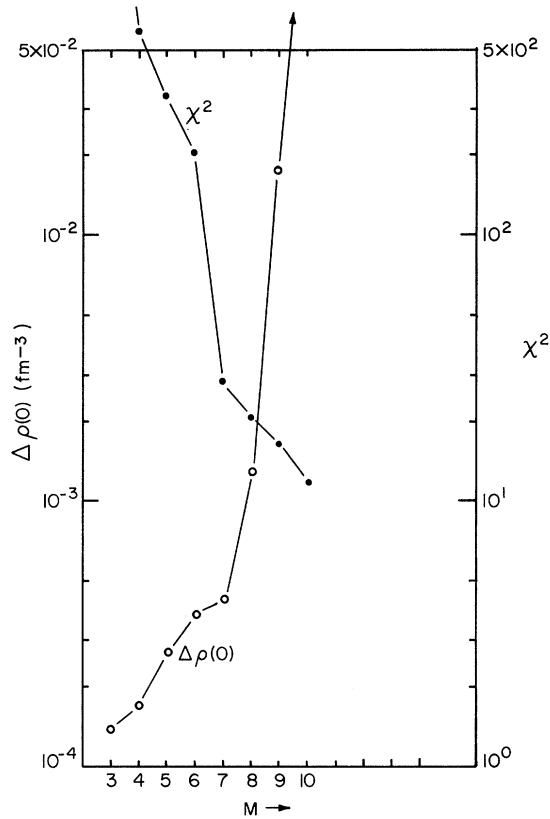


FIG. 1. χ^2 and $\Delta\rho(0)$ the error in the density at $r=0$, for ${}^3\text{He}$, as a function of the number of model states M . The expansion used is the series of cosines (6.1) with $r_0=5.0$ fm. No additional assumptions have been made about the form factor outside of the measured region. When $M=7$ or 8 the density obtained is very close to the density shown in Fig. 4. The errors obtained are unrealistically small, however. The divergence of $\Delta\rho(0)$ begins at $M=q_{\text{max}}r_0/\pi$, where q_{max} is the maximum measured momentum transfer (4.5 fm^{-1}).

mined. A space with more than eight cosines contains states which almost do not overlap with the measured region. The coefficients for such states cannot be determined well and $\Delta\rho$ becomes very large.

The situation is now as described at the end of Sec. 3. We have determined the density using a model space which is not disproved by the present experiment. As the new measurements are not immediately available we shall test the credibility of our result by: (a) simulating a null experiment and (b) trying model spaces different than the cosine model space. Starting with (a) let us consider the semilog plot $f(q)$, as in Fig. 2. Here we see that $f(q)$ falls rapidly and we imagine that it will be limited by an exponential such as the straight line in Fig. 2. We therefore introduce fictitious data: $f(q_i)=0$ with σ_i =value from

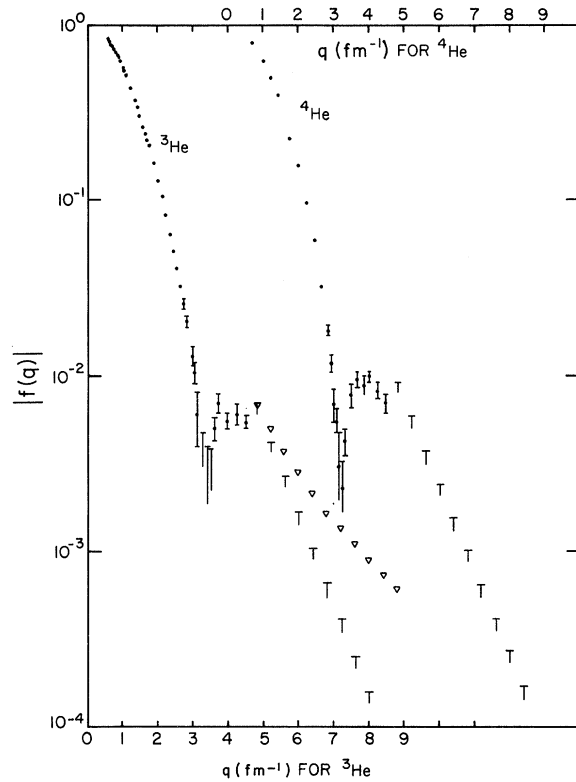


FIG. 2. The absolute value of the experimental form factor for ${}^3\text{He}$ and for ${}^4\text{He}$ as a function of momentum transfer q . Outside of the measured region we have introduced fictitious data with $f(q_i)=0$ and with error indicated by T marks. The T marked errors follow the "exponential assumption" and fall on a straight line. The ∇ marked errors follow the " q^{-4} assumption." These errors were adjusted to be identical at $q=4.8\text{ fm}^{-1}$. In each case the fictitious data go out to $q_{\text{max}}=8.8\text{ fm}^{-1}$.

TABLE I. Coefficients of the cosine series (6.1) for the densities of ${}^3\text{He}$ and ${}^4\text{He}$.

m	${}^3\text{He}$	a_m	${}^4\text{He}$
1	0.2769 - 1		0.2980 - 1
2	0.1806 - 1		0.1981 - 1
3	0.7633 - 2		0.8228 - 2
4	0.1621 - 2		0.1140 - 2
5	-0.7113 - 3		-0.1441 - 2
6	-0.1149 - 2		-0.1574 - 2
7	-0.7821 - 3		-0.8809 - 3
8	-0.3062 - 3		-0.2498 - 3
9	-0.3474 - 4		0.7280 - 5
10	0.1246 - 4		0.4543 - 5
11	-0.3367 - 5		-0.1700 - 5
12	0.1080 - 5		0.1344 - 5

straight line, for q values separated by 0.4 fm^{-1} . The values at $q=4.8(0.4)8.8$ are used.

Since $r_0 = 5 \text{ fm}$ we do not need to introduce q values closer than 0.4 fm^{-1} because this spacing satisfies the rule $\Delta q \leq \pi/r_0 \approx 0.6 \text{ fm}^{-1}$. We call this assumption the "exponential assumption." We wish to emphasize that the introduction of this assumption about $f(q)$ does not influence its functional form in any explicit way. It merely influences it to be not larger than the error introduced but allows all sorts of oscillations or other behavior so long as the magnitude of $f(q)$ is limited. [Actually the frequency of oscillation of $f(q)$ is also limited because of the assumption that $\rho(r) = 0$ for $r > 5.0 \text{ fm}$.] The exponential assumption simulates a conceivable null experiment. In practice the value of $f(q)$ in this region becomes rather small and therefore $\rho(r)$ is smoother than would be indicated by the error bars (Fig. 4). We believe the smoothness of $\rho(r)$ is a result of the ease with which a fit can be found with very small $f(q)$ outside the measured region. The error bars on $\rho(r)$ are a better indication of our imperfect knowledge in the large q region than the lack of structure in

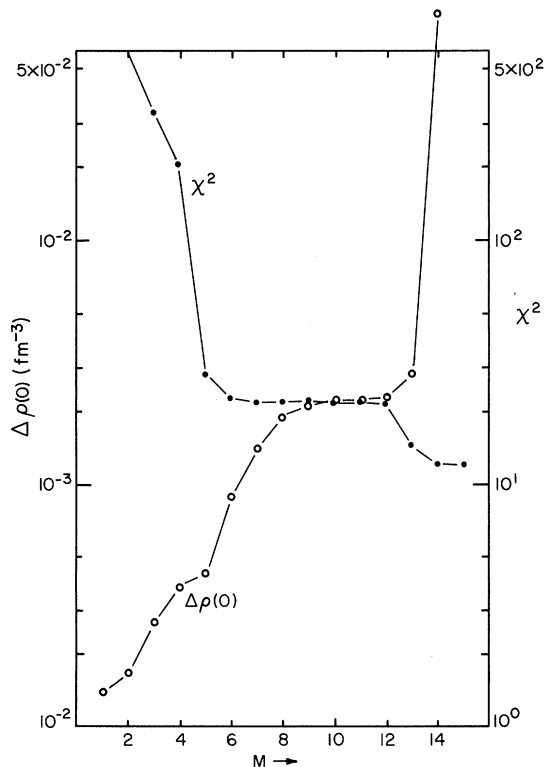


FIG. 3. The same as Fig. 1 except for the inclusion of the fictitious data above $q=4.5 \text{ fm}^{-1}$. The errors on these added points follow the exponential assumption shown in Fig. 2. $\Delta\rho(0)$ and χ^2 now both reach a plateau before $\Delta\rho(0)$ diverges and χ^2 lowers. The divergence here and in Fig. 1 occurs when $M = q_{\max} r_0 / \pi$.

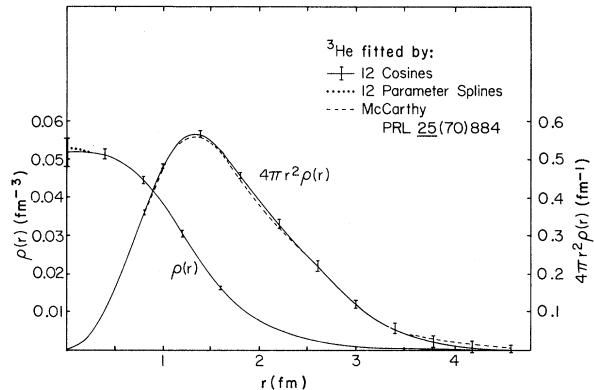


FIG. 4. Densities of ${}^3\text{He}$ determined with 12-cosine series, with 12-parameter splines, and as given by J.S. McCarthy *et al.*, Phys. Rev. Lett. 25, 884 (1970). Both $\rho(r)$ and $4\pi r^2 \rho(r)$ are shown. The normalization in this and in the following figures is $\int \rho(r) 4\pi r^2 dr = 1$. The error bars are uncorrelated errors for the 12-cosine series fit. (This density and error are also shown in Fig. 8.) χ^2 for the fit is 24. The errors for the spline function fit are similar to those shown above. The small difference between the spline and the cosine fit is probably a result of the fact that the spline functions were not constrained to have slope $d\rho/dr = 0$ at $r = 0$.

$\rho(r)$. Introducing this new data from the exponential assumption we find a χ^2 , $\Delta\rho(0)$ versus M plot as in Fig. 3. Here χ^2 reaches a plateau and $\Delta\rho(0)$ also has a definite plateau. This plateau's value is characteristic of the errors introduced in the fictitious data. The curve for $\Delta\rho(0)$ goes up sharply when $M = (r_0 q_{\max}) / \pi = 14$, q_{\max} now being 8.8 fm^{-1} instead of the measured $q_{\max} = 4.5 \text{ fm}^{-1}$. The same simple expression from Fourier transforms thus explains the location of the divergence of $\Delta\rho(0)$ in both Figs. 1 and 3. The plateau could clearly be made to extend as far as one wants by introducing

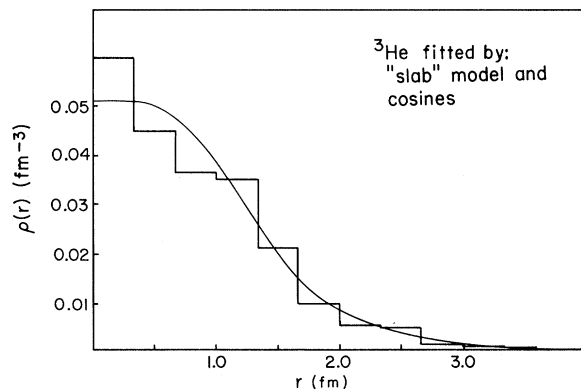


FIG. 5. Charge density of ${}^3\text{He}$ as fitted by the slab model and as fitted by the 12 cosines. The form factor derived from the slab model fits the measured points well but we find it has a rather unacceptable character outside the measured region, see Fig. 6.

data at larger and larger q 's. We will not learn much this way and use the alternative device of cutting off the cosine series at $M=12$ thus cutting off $f(q)$ in a less controlled but surely satisfactory way: We are prepared to believe for now that $M=12$ is a good model space.

Figure 4 shows the ${}^3\text{He}$ charge distribution and its errors expanded in a cosine series with $M=12$ when using the exponential assumption from Fig. 2. Table I gives the coefficients of the cosine series for this case. There may be some reasonable doubt as to the validity of the exponential assumption because it cuts off $f(q)$ somewhat rapidly. We have therefore considered the possibility that the charge distribution's Fourier transform goes down more slowly than this. It can be shown that if the charge distribution is no more singular than expected from a discontinuous second derivative (which is about as severe a discontinuity as could be entertained on physical grounds) then $f(q)$ must

fall asymptotically like q^{-4} .

We therefore also considered a limit in the form of errors on $f(q)$ for q on the points 4.8(0.4)8.8 as before but now making the standard deviations from zero proportional to q^{-4} . See the triangular points in Fig. 2. This is called the q^{-4} assumption. The resulting $\rho(r)$ is almost identical to that shown for the cosine series in Fig. 4. The errors $\Delta\rho(r)$ with this q^{-4} assumption and with the exponential assumption, used for calculating the density in Fig. 4, are compared in Fig. 5.

As stated earlier we shall discuss now fits obtained with the different model spaces. We found that sets of continuous functions give nearly identical results. An example is in Fig. 4 where $\rho(r)$ obtained with the set of cubic spline functions (Appendix) is compared with the cosine series expansion of $\rho(r)$. In both fits we used the exponential assumption. Similar results has been obtained with a power series on the interval $(0, r_0)$. The assumption that the density and its first few derivatives are continuous is unobjectionable and therefore only continuous functions should be used in final fitting. It is instructive, however, to see if good fits can be obtained with functions which are not assumed continuous or even are explicitly discontinuous. It would be disturbing if a good fit could be obtained with $\rho(r)$ having a very irregular shape. It would suggest that our method cannot discern between different shapes.

We shall consider now unspline functions. They are polynomials of the order N_k inside of fixed intervals. At the boundary points between the intervals the unspline can be continuous or discontinuous depending on N_k and the expansion coeffi-

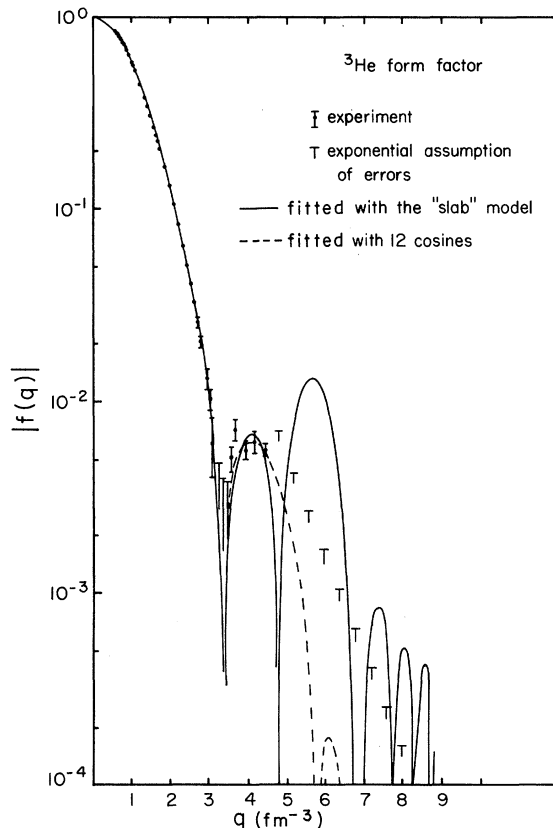


FIG. 6. The absolute values of the form factor as derived from the slab model shown in Fig. 6 and from the cosine model Eq. (6.1) with $M=12$. Note that the fit for the slab model is good through the measured points but breaks down outside the measured region where the form factor is as much as 5 times the maximum value we would expect from the exponential extrapolation.

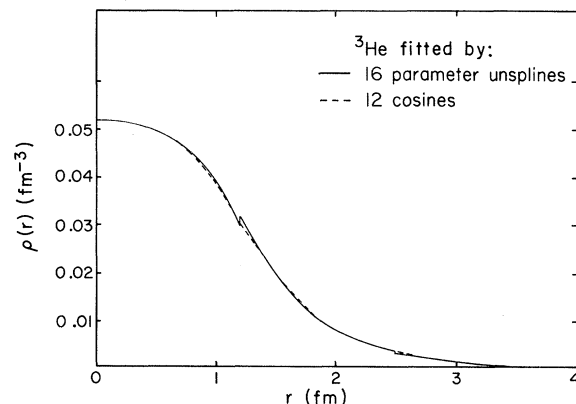


FIG. 7. The charge distribution obtained from a 16-parameter cubic unspline function compared with the 12-parameter cosines. Continuity is not demanded by the unspline functions but it is allowed. The small discontinuity leads to a rise in the form factor only outside of the region of the fictitious data, i.e., above $q=8.8 \text{ fm}^{-1}$. χ^2 for this fit is 22.

cients. For simplicity we consider equal length intervals. Further details about unsplines are given in the Appendix. For $N_k=0$ the unspline is constant inside intervals, it must be therefore discontinuous and we have a slab-shape density. With $M=15$ we find $\rho(r)$ shown in Fig. 5. Surprisingly $\chi^2=28$ is quite low in the measured region $q < 4.5 \text{ fm}^{-1}$. If the extrapolated region $4.5 < q \leq 8.8 \text{ fm}^{-1}$ is included in the calculation of χ^2 it rises to $\chi^2=135$. In Fig. 6 we see that outside $q=4.5$ the form factor is first rising and then oscillating in an unacceptable manner. We may expect that the expansion of ^{208}Pb density in terms of spherical shells³ will lead to a similar behavior of the form factor.

The last example is with $N_k=3$ and $M=16$. The density obtained is shown in Fig. 7. $\chi^2=21.2$ in the measured region $q < 4.5$ and $\chi^2=22.3$ if the extrapolated region $q \leq 8.8$ is included. The $\rho(r)$ is nearly the same as one obtained with the cosine series, except for small kinks at the boundaries between the intervals. The size of the kinks gives

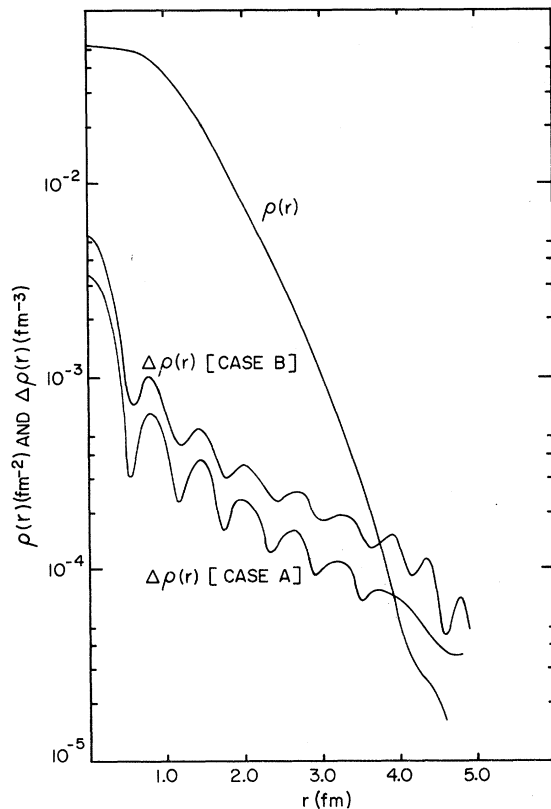


FIG. 8. The charge density $\rho(r)$ and its uncorrelated error $\Delta\rho(r)$ for ^3He as fitted by 12 cosines. $\Delta\rho(r)$ (case A) results from the exponential assumption, $\Delta\rho(r)$ (case B) results from the q^{-4} assumption discussed in Fig. 2. The dips in the error curve almost coincide with the nodes of the correlation function shown in Fig. 9.

the measure of continuity that can be deduced from the form factor known inside the limited region of $q \leq 8.8$ only.

As emphasized in Sec. 5 the errors on the charge density shown in Fig. 8 are not uncorrelated. The correlation function for the errors $g(r_1, r_2)$, as discussed, is one way of investigating these correlations. We show in Fig. 9 the particular correlation function $g(0, r)$ for ^3He fitted with 12 cosines. This indicates the correlation of the value of $\rho(r)$ with the value of $\rho(0)$. We find that most points have a very high error correlation with the point at $\rho(0)$.

We note that the dips in the error $\Delta\rho(r)$ shown in Fig. 8 correspond to the zeros of the correlation function in Fig. 9.

We note that the wavelength of the correlation function corresponds to a q of about 5.6 fm^{-1} . This is probably because the error just past $q=4.5$ is much larger than the error below that value. Furthermore the small error at $q=4.5 \text{ fm}^{-1}$ will have a restrictive effect on $f(q)$ because of the smoothness impressed by the conditions $\rho(r)=0$ outside $r=5.0 \text{ fm}$. Therefore, we do not expect $f(q)$ to have large uncertainty until q reaches at least 5.2 fm^{-1} .

We have studied ^4He in the same way and we find that because of its small radius that $f(q)$ at the largest measured⁶ q value is larger than for ^3He and as a result the extrapolated errors for $f(q)$ are larger. With exponential extrapolation as shown in Fig. 2 we obtain the charge distributions and errors for ^4He as shown in Fig. 10. Table I

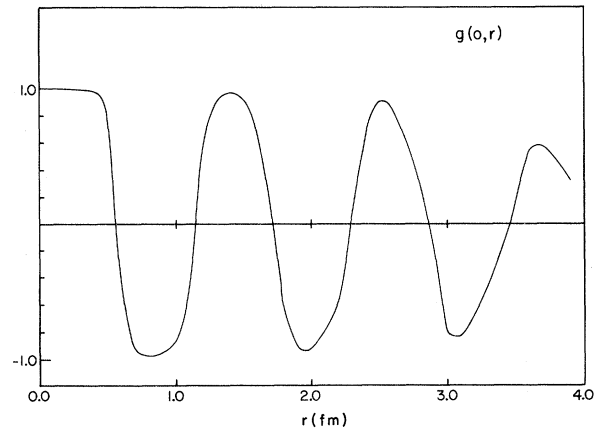


FIG. 9. The correlation function $g(0, r)$ corresponding to case A in Fig. 8. When $g(0, r)$ is near 1 or -1 the error at that point is highly correlated to the error at $r=0$. The correlations persist over a quite large range. If the density has a fixed value of $r=0$ then the error (case A) shown in Fig. 8 is reduced substantially. This is because of the strongly correlated nature of the error (except at the dips of the error curve).

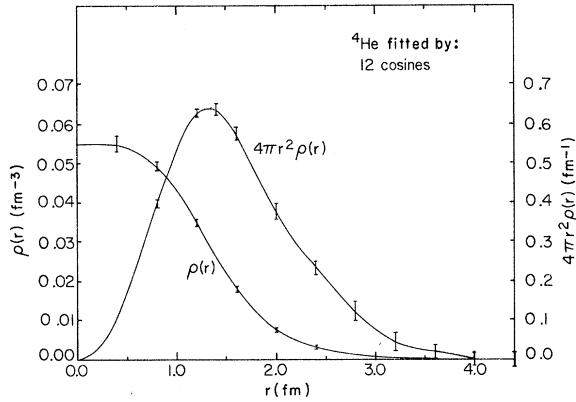


FIG. 10. Densities of ${}^4\text{He}$ determined with 12-cosine series. The uncorrelated errors are shown. χ^2 for the fit is 18.5.

shows the coefficients of the resulting cosine series corresponding to Fig. 10.

7. CONCLUSIONS

It is quite possible to analyze electron elastic scattering data in terms of rather general expansions for the density. The errors are largely determined by what kinds of limits we place on the behavior of $f(q)$ for q values larger than those measured.

We find that the most probable density $\rho(r)$ is quite insensitive to the kind of expansion used provided the assumption is made that $f(q)$ continues to fall beyond the measured region.

We found the plot of χ^2 and $\Delta\rho$ versus M (see Figs. 1 and 3) very useful in finding the dimension M of a model space. This is the M 's for which χ^2 reaches its normal range before $\Delta\rho$ becomes too large for our purpose. If such an M does not exist the model space is useless.

Since the limits on $f(q)$ are introduced by giving $f(q)=0$ with some error it is clear that even a null experiment at q values larger than the measured ones would be quite useful if it would provide a bound on $f(q)$ with limits comparable to or even somewhat larger than the measured errors on the last few points. Such bounds would not need to be taken at very many q values and could be determined with fairly wide experimental angular resolution, since $\Delta Q \approx 0.5 \text{ fm}^{-1}$ is compatible with $\rho(r)=0$ for $r \geq 5 \text{ fm}$.

ACKNOWLEDGMENTS

We wish to thank Professor D. G. Ravenhall and Professor H. McManus for stimulating conversations. We wish to acknowledge a useful conversation with Dr. J. Negele concerning the linearization of the charge density. We wish to thank Pro-

fessor J. S. McCarthy for sending the ${}^3\text{He}$ data to us. We greatly acknowledge the excellent computing facilities at the Cyclotron Laboratory of the Michigan State University.

APPENDIX

A. Spline Functions

We shall describe here an expansion of $\rho(r)$ in terms of spline functions:

$$\rho(r) = \sum_{k=1}^K a_k \varphi_k(r) + \sum_{k=1}^K b_k \eta_k(r), \quad K = \frac{1}{2}M. \quad (\text{A1})$$

We want $\rho(r)$ and its first derivative $\rho'(r)$ to be continuous on the interval (r_1, r_k) . Moreover, for a given set of points

$$r_1 < r_2 < \dots < r_i \dots < r_k \quad (\text{A2})$$

we want to have

$$\begin{aligned} \rho(r_i) &= a_i, \\ \rho'(r_i) &= b_i. \end{aligned} \quad (\text{A3})$$

The (A3) will be true if the functions $\varphi_i(r)$ and $\eta_i(r)$ fulfill the following conditions:

$$\begin{aligned} \varphi_i(r) &= \begin{cases} 0 & \text{for } r \leq r_{i-1}, r \geq r_{i+1} \\ 1 & \text{for } r = r_i; \end{cases} \\ \varphi_i'(r) &= 0 \quad \text{for } r = r_{i-1}, r_i, r_{i+1}; \\ \eta_i(r) &= 0 \quad \text{for } r \leq r_{i-1}, r = r_i, r \geq r_{i+1}; \\ \eta_i'(r) &= \begin{cases} 0 & \text{for } r = r_{i-1}, r = r_{i+1} \\ 1 & \text{for } r = r_i. \end{cases} \end{aligned} \quad (\text{A4})$$

There are many functions with such properties. We use a simple representation in terms of cubic polynomials:

$$\begin{aligned} \varphi_i(r) &= \begin{cases} f\left(\frac{r-r_i}{r_{i+1}-r_i}\right) & \text{for } r_1 \leq r \leq r_{i+1} \\ f\left(\frac{r-r_i}{r_{i-1}-r_i}\right) & \text{for } r_{i-1} \leq r \leq r_i \end{cases} \\ \eta_i(r) &= \begin{cases} (r_{i+1}-r_i)g\left(\frac{r-r_i}{r_{i+1}-r_i}\right) & \text{for } r_i \leq r \leq r_{i+1} \\ (r_{i-1}-r_i)g\left(\frac{r-r_i}{r_{i-1}-r_i}\right) & \text{for } r_{i-1} \leq r \leq r_i, \end{cases} \end{aligned} \quad (\text{A5})$$

where

$$\begin{aligned} f(x) &= 2x^3 - 3x^2 + 1, \\ g(x) &= x^3 - 2x^2 + x. \end{aligned} \quad (\text{A6})$$

B. Unspline Functions

Let us divide the region $0 \leq r \leq r_0$ into N_i equal intervals of length $D = r_0/N_i$ and let us call the midpoint of the i 's interval r_i .

We shall consider now the following expansion of $\rho(r)$:

$$\rho(r) = \sum_{i=1}^{N_i} \sum_{k=0}^{N_k} a_{ik} [\varphi_i(r)]^k, \quad (\text{A7})$$

where

$$\varphi_i(r) = \begin{cases} r - r_i & \text{if } r_i - \frac{1}{2}D \leq r < r_i + \frac{1}{2}D \\ 0 & \text{otherwise.} \end{cases} \quad (\text{A8})$$

Inside of each interval $\rho(r)$ is a polynomial of degree N_k . No continuity conditions are imposed on $\rho(r)$ at boundaries between intervals. However form (A7) allows $\rho(r)$ and/or its derivatives to be continuous. With the increasing N_k higher degree of continuity (that is in higher derivatives) at boundaries is possible. For $N_k = 0$ we have the "slab" model and unless $\rho(r)$ is constant it must be discontinuous. A typical shape is shown in Fig. 5. For $N_k = 1$, ρ and/or its derivatives may be continuous.

*Work supported in part by the National Science Foundation.

¹Actually the measured quantity in any case is the cross section which is a square of a linear functional even in Born approximation. However, we have assumed that the derived $f(q)$ and its error can be taken as input data for our calculation when Born approximation is valid.

²H. R. Collard *et al.*, *Nuclear Radii* (Springer, Berlin, 1967).

³F. Friedrich and F. Lenz, *Nucl. Phys.* **A183**, 523 (1972).

⁴Equations (3.4), (3.5), and (3.6) have proved quite use-

ful. They are not proved here, but they express generally accepted ideas about Fourier transforms.

⁵Note that in the case of linearized functionals

$$P_{im} = \lim_{\Delta a \rightarrow 0} [F_i\{\rho_0(r) + \Delta a M_m(r)\} - F_i\{\rho_0(r)\}] / \Delta a$$

which is easily determined from a program for cross section in terms of charge density provided we use a finite Δa .

⁶ $\Delta\rho(r)$ may be infinite.

⁷J. S. McCarthy, private communication.

⁸R. F. Frisch *et al.*, *Phys. Rev.* **160**, 874 (1967).